Self-Organization of Polymerizable Bolaamphiphiles Bearing Diacetylene Mesogenic Group

Shouchun Yin, Bo Song, Guanqing Liu, Zhiqiang Wang, and Xi Zhang*

Key Lab of Optoelectronics and Molecular Engineering, Department of Chemistry, Tsinghua University, Beijing 100084, People's Republic of China

Received February 1, 2007. In Final Form: March 16, 2007

We report herein the synthesis of a series of polymerizable bolaamphiphiles containing a diacetylene group and mesogenic unit and their self-organization behaviors in bulk and at interface. The polymerizable bolaamphiphiles are noted as DPDA-*n*, where *n* refers to the spacer length of alkyl chain. DPDA-10 with suitable spacer length can self-organize into stable cylindrical micellar nanostructures, and these nanostructures have preferred orientation regionally when adsorbed at the mica/water interface. It is confirmed that the micellar nanostructure of DPDA-10 can be polymerized both in the bulk solution and in the film by UV irradiation. The emission property of DPDA-10 after UV irradiation has been significantly enhanced in comparison to that before polymerization, which may be due to the extension of the conjugated system arising from the transformation of the diacetylene group into polydiacetylene upon polymerization. In addition, the self-organization of DPDA-*n* is dependent on the spacer length. DPDA-7 with a short spacer length forms an irregular flat sheet structure with many defects; DPDA-15 with a long spacer length forms rodlike micellar structures. Thus, this work may provide a new approach for designing and fabricating organic functional nanostructured materials.

Introduction

Amphiphiles can self-organize into micellar structures with defined size and shape in bulk solutions,[1] and these structures can adsorb onto a solid/liquid interface forming ordered surface micelles. Although the conventional surfactants such as hexadecyltrimethylammonium bromide (CTAB) can form surface spherical, cylindrical, or hemicylindrical micelles, and bilayer structures at a solid/liquid interface,[2] these well-defined structures will be destroyed due to inherent dynamics and fluid after the substrate is taken out from the solution. Engineering robustness is, however, required for the design and synthesis of stable interfacial structures so that they may be used in applications such as templates for making nanostructured materials and mimicking biomineralization processes.

In the past few years, by introducing mesogenic groups into bolaamphiphiles, we have obtained stable nanostructures with different morphologies in the dry state, such as stripes, spaghettis, and discs, because the mesogenic group may enhance the intermolecular interactions among amphiphiles.[3] We have also adopted other effective methods to stabilize surface micelles by introducing polymerizable groups into amphiphiles.[4] For example, the preformed wormlike micellar structures at the mica/water interface can be preserved well by γ-ray-initiated polymerization[4a] or ring-opening polymerization under mild conditions.[4b]

To combine the above two methods for stabilizing nanostructures, herein we present the design and synthesis of bolaamphiphiles containing a polymerizable mesogenic group of the diphenylbutadiynyl moiety. Diacetylene monomers are known to undergo topochemical polymerization upon irradiation by UV light or γ-rays to form an eneyne alternated conjugation polydiacetylene,[5] which are used in the fields of nonlinear optics,[6] emitting material,[7] conductivity material,[8] colorimetric sensors,[9] and photolithography[10] because of the formed polydiacetylene, being a large quasi one-dimensional π-conjugated system. It is anticipated that these bolaamphiphiles we synthesized can self-organize to form stable nanostructures due to the introduction of the mesogenic diphenylbutadiynyl group, and these nano-

* To whom correspondence may be addressed. Fax: +86-010-62771149. E-mail: xi@mail.tsinghua.edu.cn.

(1) (a) Ringsdorf, H.; Schlarb, B.; Venzmer, J. *Angew. Chem., Int. Ed. Engl.* **1988**, *27*, 113. (b) Ahlers, M.; Mueller, W.; Reichert, A.; Ringsdorf, H.; Venzmer, J. *Angew. Chem., Int. Ed. Engl.* **1990**, *29*, 1269. (c) Kunitake, T. *Angew. Chem., Int. Ed. Engl.* **1992**, *31*, 709.

(2) (a) Manne, S.; Gaub, H. E. *Science* **1995**, *270*, 1480. (b) Jaschke, M.; Butt, H. J.; Gaub, H. E.; Manne, S. *Langmuir* **1997**, *13*, 1381. (c) Lamont, R. E.; Ducker, W. A. *J. Am. Chem. Soc.* **1998**, *120*, 7602. (d) Ducker, W. A.; Wanless, E. J. *Langmuir* **1999**, *15*, 160. (e) Patrick, H. N.; Warr, G. G.; Manne, S.; Aksay, I. A. *Langmuir* **1999**, *15*, 1685.

(3) (a) Gao, S.; Zou, B.; Chi, L. F.; Fuchs, H.; Sun, J. Q.; Zhang, X.; Shen, J. C. *Chem. Commun.* **2000**, 1273. (b) Zou, B.; Wang, L. Y.; Wu, T.; Zhao, X. Y.; Wu, L. X.; Zhang, X.; Gao, S.; Gleiche, M.; Chi, L. F.; Fuchs, H. *Langmuir* **2001**, *17*, 3682. (c) Zou, B.; Wang, M. F.; Qiu, D. L.; Zhang, X.; Chi, L. F.; Fuchs, H. *Chem. Commun.* **2002**, 1008. (d) Wang, M. F.; Qiu, D. L.; Zou, B.; Wu, T.; Zhang, X. *Chem.*−*Eur. J.* **2003**, *9*, 1876. (e) Song, B.; Wang, Z. Q.; Chen, S. L.; Zhang, X.; Fu, Y.; Smet, M.; Dehaen, W. *Angew. Chem., Int. Ed.* **2005**, *44*, 4731. (f) Song, B.; Wang, Z. Q.; Zhang, X. *Pure Appl. Chem.* **2006**, *78*, 1015. (g) Song, B.; Wei, H.; Wang, Z. Q.; Zhang, X.; Smet, M.; Dehaen, W. *Adv. Mater.* **2007**, *19*, 416.

(4) (a) Zhang, X.; Wang, M. F.; Wu, T.; Jiang, S. C.; Wang, Z. Q. *J. Am. Chem. Soc.* **2004**, *126*, 6572. (b) Liu, F.; Wang, M. F.; Wang, Z. Q.; Zhang, X. *Chem. Commun.* **2006**, 1610.

(5) (a) Enkelmann, V. *Adv. Polym. Sci.* **1984**, *63*, 91. (b) Tieke, B. *Adv. Polym. Sci.* **1985**, *71*, 80.

(6) (a) Paley, M. S.; Frazier, D. O.; Abdeldeyem, H.; Armstrong, S.; McManus, S. P. *J. Am. Chem. Soc.* **1995**, *117*, 4775. (b) Jenkins, I. H.; Kar, A. K.; Lindsell, W. E.; Murray, C.; Preston, P. N.; Wang, C. H.; Wherrett, B. S. *Macromolecules* **1996**, *29*, 6365. (c) Huggins, K. E.; Son, S.; Stupp, S. I. *Macromolecules* **1997**, *30*, 5305. (d) Sarkar, A.; Okada, S.; Nakanishi, H.; Matsuda, H. *Macromolecules* **1998**, *31*, 9174. (e) He, J. A.; Yang, K.; Kumar, J.; Tripathy, S. K.; Samuelson, L. A.; Oshikiri, T.; Katagi, H.; Kasai, H.; Okada, S.; Oikawa, H.; Nakanashi, H. *J. Phys. Chem. B* **1999**, *103*, 11050.

(7) (a) Musso, G. F.; Ottonelli, M.; Alloisio, M.; Moggio, I.; Comoretto, D.; Cuniberti, C.; Dellepiane, G. *J. Phys. Chem. A* **1999**, *103*, 2857. (b) Aida, T.; Tajima, K. *Angew. Chem., Int. Ed.* **2001**, *40*, 3803. (c) Gan, H. Y.; Liu, H. B.; Li, Y. J.; Zhao, Q.; Li, Y. L.; Wang, S.; Jiu, T. G.; Wang, N.; He, X. R.; Yu, D. P.; Zhu, D. B. *J. Am. Chem. Soc.* **2005**, *127*, 12452.

(8) (a) Savenije, T. J.; Warman, J. M.; Barentsen, H. M.; Dijk, M.; Zuilhof, H.; Sudhoelter, E. J. R. *Macromolecules* **2000**, *33*, 60. (b) Hoofman, R. J. O. M.; Gelinck, G. H.; Siebbeles, L. D. A.; Haas, M. P.; Warman, J. M.; Bloor, D. *Macromolecules* **2000**, *33*, 9289. (c) Takami, K.; Mizuno, J.; Megumi, A.; Saito, A.; Aono, M.; Kuwahara, Y. *J. Phys. Chem. B* **2004**, *108*, 16353.

(9) (a) Mowery, M. D.; Smith, A. C.; Evans, C. E. *Langmuir* **2000**, *16*, 5998. (b) Morigaki, K.; Baumgart, T.; Offenhaeusser, A.; Knoll, W. *Angew. Chem., Int. Ed.* **2001**, *40*, 172. (c) Morigaki, K.; Baumgart, T.; Jonas, U.; Offenhäusser, A.; Knoll, W. *Langmuir* **2002**, *18*, 4082. (d) Kim, B. G.; Kim, S.; Seo, J.; Oh, N. K.; Zin, W. C.; Park, Y. S. *Chem. Commun.* **2003**, 2306.

10.1021/la700281f CCC: $37.00
Published on Web 04/26/2007

structures can be further polymerized into polydiacetylene, thus providing a way for fabricating functional polymer nanomaterials.

Experimental Section

Materials. 4-ethynylbenzyl alcohol, 8-bromooctanoic acid, 11-bromoundecanoic acid, and 16-bromohexadecanoic acid were purchased from Aldrich. THF and toluene were distilled from sodium benzophenone ketyl, and triethylamine was distilled from potassium hydroxide prior to use.

Instruments and Methods. The ^{1}H NMR spectra were recorded on a JEOL ECA-300 apparatus. Mass spectra (MS) were recorded on a LTQ LC/MS/MS apparatus. UV−vis spectra were measured with a HITACHI U-3010 spectrometer. The solutions (1.0×10^{-3} M) were diluted 10-fold before the absorption spectrum was recorded. FTIR spectroscopy was performed on a Bruker IFS 66v/s spectrophotometer. The samples were dropped onto the CaF_2 and measured in vacuum. Fluorescence emission spectra were recorded with a Perkin-Elmer LS 55 spectrophotometer. The solutions (1.0×10^{-3} M) were diluted 10-fold before the emission spectrum was recorded.

Synthesis of 1,4-Bis(4-hydroxymethylenephenyl)butadiyne. 528 mg (4 mmol) 4-ethynylbenzyl alcohol was added to a solution of 143 mg (1.44 mmol) copper(I) chloride in 8 mL pyridine, into which oxygen was bubbled. Then, the mixture was stirred overnight at room temperature. After pyridine was removed under reduced pressure, the residue was dissolved into 100 mL ethyl acetate and washed with 5% acetic acid until the blue color disappeared. The resultant organic layer was dried over anhydrous magnesium sulfate, filtered, and evaporated. The residue was purified by SiO_2 column chromatography using a mixture of ethyl acetate/petroleum ether (1:1 v/v) as eluent to give a pale yellow solid. Yield: 67%. ^{1}H NMR (300 MHz, DMSO-d_6) δ (ppm): 7.56 (4H, d, J = 8.2 Hz, Ar−H ortho to C≡C), 7.37 (4H, d, Ar−H meta to C≡C), 4.52 (4H, s, CH_2OH), 3.85 (2H, s, CH$_2$OH).

Synthesis of 1,4-Bis(4-[({[7-bromooctayl]carbonyl}oxy)-methylene]phenyl)butadiyne. In a two-necked 100 mL round-bottom flask under nitrogen were dissolved 555 mg (2.5 mmol) 8-bromooctanoic acid and 6 mL $SOCl_2$ in 10 mL anhydrous toluene. The mixture was refluxed for 5 h. The solvent and excessive $SOCl_2$ were removed under reduced pressure, and the residue was dissolved in 6 mL anhydrous THF. Then, this solution was added dropwise to a stirred solution of 315 mg (1.2 mmol) 1,4-bis(4-hydroxymethylphenyl)butadiyne and 0.35 mL triethylamine (2.5 mmol) in 10 mL THF. After stirring at room temperature for 1 h, the mixture was refluxed for 48 h. Then, the solvent was removed under reduced pressure, and the crude product was purified by SiO_2 column chromatography using a mixture of ethyl acetate/petroleum ether (1:3 v/v) as eluent to give a pale yellow solid in 41% yield. ^{1}H NMR (300 MHz, $CDCl_3$) δ (ppm): 7.52 (4H, d, J = 8.2 Hz, Ar−H ortho to C≡C), 7.32 (4H, d, Ar−H meta to C≡C), 5.11 (4H, s, ArCH_2O), 3.39 (4H, t, J = 7.0 Hz, Br(CH$_2$)$_6$CH_2), 2.36 (4H, t, J = 7.5 Hz, BrCH_2(CH$_2$)$_6$), 1.84 (4H, m, Br(CH$_2$)$_5$CH_2CH$_2$), 1.65 (4H, m, BrCH$_2$CH_2(CH$_2$)$_5$), 1.51−1.21 (12H, m, Br(CH$_2$)$_2$(CH_2)$_3$(CH$_2$)$_2$).

A similar procedure was adopted for the synthesis of 1,4-bis(4-[({[10-bromodecatyl]carbonyl}oxy)methylene]phenyl)butadiyne and 1,4-bis(4-[({[15-bromopentadecyl]carbonyl}oxy)methylene]phenyl)-butadiyne.

Synthesis of 1,4-Bis(4-[({[10-bromodecatyl]carbonyl}oxy)-methylene]phenyl)butadiyne. Pale yellow solid. Yield: 58%. ^{1}H NMR (300 MHz, $CDCl_3$) δ (ppm): 7.51 (4H, d, J = 8.0 Hz, Ar−H ortho to C≡C), 7.31 (2H, d, Ar−H meta to C≡C), 5.11 (4H, s, ArCH_2O), 3.40 (4H, t, J = 6.9 Hz, Br(CH$_2$)$_9$CH_2), 2.36 (4H, t, J = 7.6 Hz, BrCH_2(CH$_2$)$_9$), 1.84 (4H, m, Br(CH$_2$)$_8$CH_2CH$_2$), 1.63 (4H, m, BrCH$_2$CH_2(CH$_2$)$_8$), 1.52−1.20 (24H, m, Br(CH$_2$)$_2$(CH_2)$_6$(CH$_2$)$_2$).

Synthesis of 1,4-Bis(4-[({[15-bromopentadecyl]carbonyl}oxy)-methylene]phenyl)butadiyne. Pale yellow solid. Yield: 52%. ^{1}H NMR (300 MHz, $CDCl_3$) δ (ppm): 7.52 (4H, d, J = 8.2 Hz, Ar−H ortho to C≡C), 7.32 (4H, d, Ar−H meta to C≡C), 5.11 (4H, s, ArCH_2O), 3.41 (4H, t, J = 6.8 Hz, Br(CH$_2$)$_{14}$CH_2), 2.37 (4H, t, J = 7.6 Hz, BrCH_2(CH$_2$)$_{14}$), 1.86 (4H, m, Br(CH$_2$)$_{13}$CH_2CH$_2$), 1.63 (4H, m, BrCH$_2$CH_2(CH$_2$)$_{13}$), 1.52−1.21 (44H, m, Br(CH$_2$)$_2$(CH_2)$_{11}$-(CH$_2$)$_2$).

Synthesis of 1,4-Bis(4-[({[7-(1-pyridinium)octayl]carbonyl}-oxy)methylene]phenyl)butadiyne (denoted DPDA-7). 300 mg (0.47 mmol) 1,4-bis(4-[({[7-bromooctayl]carbonyl}oxy)methylene]-phenyl)butadiyne was dissolved in 10 mL pyridine. The solution was stirred at 70 °C for 48 h under nitrogen. After cooling to room temperature, the solvent was removed under reduced pressure. The residue was dissolved in 3 mL methanol and then added dropwise to 60 mL toluene to give a pink solid precipitation. The crude product was redissolved in acetonitrile and precipitated twice in diethyl ether to give a white solid. Yield: 78%. ^{1}H NMR (300 MHz, DMSO-d_6) δ (ppm): 9.06 (4H, d, J = 5.9 Hz, Ar−H ortho to N$^+$), 8.60 (2H, t, J = 7.7 Hz, Ar−H para to N$^+$), 8.15 (4H, d, Ar−H meta to N$^+$), 7.61 (4H, d, J = 7.9 Hz, Ar−H ortho to C≡C), 7.41 (4H, d, Ar−H meta to C≡C), 5.12 (4H, s, ArCH_2O), 4.58 (4H, t, J = 7.2 Hz, CH_2(CH$_2$)$_6$COO), 2.36 (4H, t, (CH$_2$)$_6$CH_2COO), 1.91 (4H, m, CH$_2$CH_2(CH$_2$)$_5$COO), 1.52 (4H, m, (CH$_2$)$_5$CH_2CH$_2$COO), 1.42−1.12 (12H, m, (CH$_2$)$_2$(CH_2)$_3$(CH$_2$)$_2$COO). ESI-MS: m/z 335.57 [MH]$^+$.

1,4-Bis(4-[({[10-(1-pyridinium)decatyl]carbonyl}oxy)methylene]-phenyl)butadiyne (DPDA-10) and 1,4-bis(4-[({[15-(1-pyridinium)-pentadecyl]carbonyl}oxy)methylene]phenyl)butadiyne (DPDA-15) were synthesized by the same procedure above.

Synthesis of 1,4-Bis(4-[({[10-(1-pyridinium)decatyl]carbonyl}-oxy)methylene]phenyl)butadiyne (denoted DPDA-10). White solid. Yield: 84%. ^{1}H NMR (300 MHz, DMSO-d_6) δ (ppm): 9.08 (4H, d, J = 5.5 Hz, Ar−H ortho to N$^+$), 8.59 (2H, t, J = 7.7 Hz, Ar−H para to N$^+$), 8.14 (4H, d, Ar−H meta to N$^+$), 7.60 (4H, d, J = 8.0 Hz, Ar−H ortho to C≡C), 7.41 (4H, d, Ar−H meta to C≡C), 5.11 (4H, s, ArCH_2O), 4.59 (4H, t, J = 7.6 Hz, CH_2(CH$_2$)$_9$-COO), 2.35 (4H, t, J = 7.6 Hz, (CH$_2$)$_9$CH_2COO), 1.90 (4H, m, CH$_2$CH_2(CH$_2$)$_8$COO), 1.52 (4H, m, (CH$_2$)$_8$CH_2CH$_2$COO), 1.35−1.12 (24H, m, (CH$_2$)$_2$(CH_2)$_6$(CH$_2$)$_2$COO). ESI-MS: m/z 377.62 [MH]$^+$.

Synthesis of 1,4-Bis(4-[({[15-(1-pyridinium)pentadecyl]-carbonyl}oxy)methylene]phenyl)butadiyne (denoted DPDA-15). White solid. Yield: 92%. ^{1}H NMR (300 MHz, DMSO-d_6) δ (ppm): 9.06 (4H, d, J = 5.5 Hz, Ar−H ortho to N$^+$), 8.59 (2H, t, J = 7.9 Hz, Ar−H para to N$^+$), 8.14 (4H, d, Ar−H meta to N$^+$), 7.60 (4H, d, J = 8.0 Hz, Ar−H ortho to C≡C), 7.41 (4H, d, Ar-H meta to C≡C), 5.11 (4H, s, ArCH_2O), 4.57 (4H, t, J = 7.2 Hz, CH_2(CH$_2$)$_{14}$-COO), 2.34 (4H, t, J = 7.6 Hz, (CH$_2$)$_{14}$CH_2COO), 1.89 (4H, m, CH$_2$CH_2(CH$_2$)$_{13}$COO), 1.52 (4H, m, (CH$_2$)$_{13}$CH_2CH$_2$COO), 1.34−1.10 (44H, m, (CH$_2$)$_2$(CH_2)$_{11}$(CH$_2$)$_2$COO). ESI-MS: m/z 447.75 [MH]$^+$.

Atomic Force Microscopy (AFM). A commercial multimode Nanoscope IV AFM was employed to characterize the surface structure. AFM images were recorded in situ and ex situ at the solid/liquid interface at room temperature. In situ AFM images were obtained with a tapping mode in fluid; ex situ AFM images were obtained with tapping mode in air. Sharpened Si_3N_4 cantilevers were used for the tapping mode in fluid; Si cantilevers were used for the tapping mode in air. All cantilevers were purchased from Veeco company. Muscotive mica (Plannet GmbH, Germany) was freshly cleaved before immersion in the aqueous solution of the amphiphile at a concentration, above the critical micelle concentration (cmc). Before the ex situ AFM images were recorded, the mica was first incubated in the DPDA aqueous solution for 30 min, then taken out from the solution, immediately dip-rinsed in distilled water, and

(10) (a) Okada, S.; Peng, S.; Spevak, W.; Charych, D. *Acc. Chem. Res.* **1998**, *31*, 229. (b) Jonas, U.; Shah, K.; Norvez, S.; Charych, D. H. *J. Am. Chem. Soc.* **1999**, *121*, 4580. (c) Kolusheva, S.; Shahal, T.; Jelinek, R. *J. Am. Chem. Soc.* **2000**, *122*, 776. (d) Lu, Y. F.; Yang, Y.; Sellinger, A.; Lu, M. C.; Huang, J. M.; Fan, H. Y.; Haddad, R.; Lopez, G.; Bums, A. R.; Sasaki, D. Y.; Shelnutt, J.; Brinker, C. J. *Nature (London)* **2001**, *410*, 913. (e) Mueller, A.; O', Brien, D. F. *Chem. Rev.* **2002**, *102*, 727. (f) Gill, I.; Ballesteros, A. *Angew. Chem., Int. Ed.* **2003**, *42*, 3264. (g) Ahn, D. J.; Chae, E. H.; Lee, G. S.; Shim, H. Y.; Chang, T. E.; Ahn, K. D.; Kim, J. M. *J. Am. Chem. Soc.* **2003**, *125*, 8976. (h) Yuan, Z. Z.; Lee, C. W.; Lee, S. H. *Angew. Chem., Int. Ed.* **2004**, *43*, 4197. (i) Rangin, M.; Basu, A. *J. Am. Chem. Soc.* **2004**, *126*, 5038. (j) Orynbayeva, Z.; Kolusheva, S.; Livneh, E.; Lichtenshtein, A.; Nathan, I.; Jelinek, R. *Angew. Chem., Int. Ed.* **2005**, *44*, 1092. (k) Ma, G. Y.; Müller, A. M.; Bardeen, C. J.; Cheng, Q. *Adv. Mater.* **2006**, *18*, 55.

Scheme 1. Synthetic Scheme of the Diacetylenic Derivatives

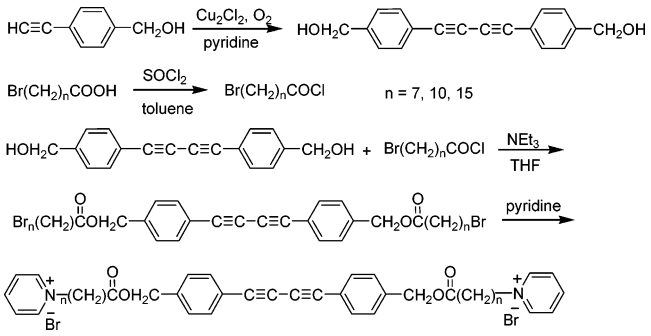

dried for at least 10 h at room temperature. Before the in situ AFM images were recorded, a mica carrying DPDA micelles, which was obtained just as above, was irradiated for 10 min with a UV fiber lamp, then placed at the AFM apparatus. A DPDA-10 aqueous solution with a concentration of 1.0×10^{-3} M after UV irradiation for 50 min was injected into the liquid cell and allowed to equilibrate for at least 1 h. The solution was held within the liquid cell by an O-ring.

UV-Initiated Polymerization. The polymerization was carried out under argon by UV irradiation using a 1 W low-pressure mercury fiber lamp. The distance between the sample and the UV lamp was 10 cm. Care was taken that the temperature never exceeded 25 °C during the polymerization procedure.

Results and Discussion

Self-Organization of DPDA-10 in Aqueous Solution. The bolaamphiphile DPDA-10 bearing a diphenylbutadiynyl group was designed and synthesized. The synthetic route was shown in Scheme 1. The diphenylbutadiynyl group has a dumbbell structure with diacetylene capped by two phenyl rings, acting as a rigid mesogenic segment to enhance the intermolecular interaction between the bolaamphiphiles, thus rendering a stable supramolecular organization. Furthermore, after polymerizing the diacetylene group to form the polydiacetylene polymer, the phenyl substituents directly attached to the polydiacetylene main backbone may enhance and modulate the optical properties of polydiacetylene due to the increase of π-delocalization through π-conjugation between the main backbone and side group. For comparison, the analogue categories with different alkyl spacers, DPDA-7 for short spacer and DPDA-15 for long spacer, are also synthesized.

To ensure whether this line of molecules has self-organization behavior in the aqueous solution, the cmc value was measured by a concentration-dependent conductivity plot. With DPDA-10 as an example, as shown in Figure 1, there is an abrupt change of the slope at 4.2×10^{-4} mol/L, corresponding to the cmc of DPDA-10. It means that the bolaamphiphile DPDA-10 can self-organize into a certain kind of micellar structures when the concentration is beyond this value.

Self-Organized Cylindrical Structure of DPDA-10. We have employed AFM to confirm the formation of micellar structures by self-organization of DPDA-10. Here, a concentration of 1.0×10^{-3} M was selected as the characterized concentration of bulk solution. The freshly cleaved mica sheet was first immersed into the solution and incubated for 30 min to allow the equilibrated adsorption of the micelles on the substrate; then, the mica sheet was taken out from the solution, immediately dip-rinsed in water, and air-dried at room temperature; at last, the fabricated sample was imaged by ex situ AFM observation. As exhibited in Figure 2b, DPDA-10 forms cylindrical micellar structures. On the mica sheet, the cylinders seem to have a preferred orientation regionally and pack parallel, though they

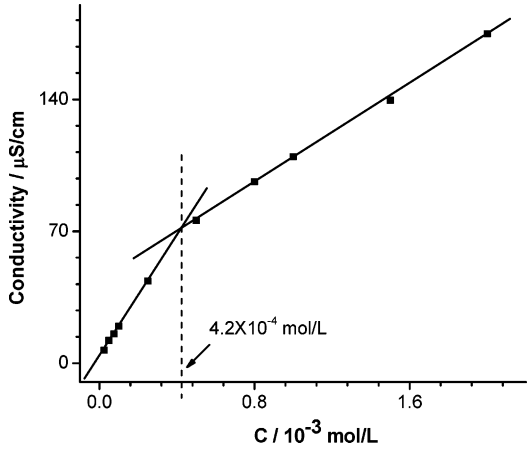

Figure 1. Dependence of the solution conductivity of DPDA-10 on concentration.

cannot cover the whole flat, leaving some places free. Statistic analysis shows that the mean spacing of ordered cylinders is approximately 6 nm, and the average thickness is about 3.2 nm. Considering that the total length of a single DPDA-10 molecule is 4.8 nm, we can deduce that the formation of the cylinder may owe to the parallel packing of the bolaamphiphile DPDA-10, with hydrophilic heads outside and hydrophobic parts inside. In situ AFM (Figure 2d) observation demonstrates the presence of similar cylindrical structures as those observed by ex situ AFM, indicating that the cylindrical structures are not formed during the air-drying process. Moreover, we have investigated the effect of the concentration on the self-organized structures and found that there is little difference in the AFM images obtained at different concentrations above the cmc.

The similar self-organization morphology did not happen to the analogue categories DPDA-15 and DPDA-7. As shown in Figure 3a, DPDA-7 forms an irregular flat sheet structure with many defects, and this structure may correspond to the collapse of DPDA-7 micelles during the drying process because of its short spacer,[11] while DPDA-15, as shown in Figure 3b, exhibits distinctly different self-organization behavior at the solid/liquid interface compared with DPDA-10, forming the rodlike micellar structures but without long-range order. It should be pointed out that the self-organization of DPDA-15 is inhibited by its poor solubility in water, since the longer the spacer length, the poorer the solubility. Therefore, an appropriate length of the flexible spacers is necessary for such bolaamphiphiles to self-organize into the well-ordered nanostructures.

Photopolymerization of DPDA-10 in the Micellar Structure. Since DPDA-10 can self-organize into micellar structure in the aqueous solution as evidenced above, we wondered if the molecules in the aggregates can undergo the topochemical polymerization by irradiation. In order to clarify this point, both UV−vis and FTIR spectroscopy were employed to follow the polymerization process. Figure 4 shows the UV−vis spectra of the photopolymerization process of the DPDA-10 aqueous solution. As shown in Figure 4, there are three absorption bands at around 294, 313, and 333 nm in the aqueous solution corresponding to the absorption of the 1,4-diphenylbutadiynyl group in DPDA-10, and there is almost no absorption after 400 nm (Figure 4, solid curve). However, after UV irradiation, a drastic change in the UV spectrum is observed (Figure 4, dashed curve). The characteristic absorption of the 1,4-diphenylbutadiynyl group of the DPDA-10 monomer becomes weaker and weaker

(11) Qiu, D. L.; Song, B.; Lin, A. L.; Wang, C. Y.; Zhang, X. *Langmuir* **2003**, *19*, 8122.

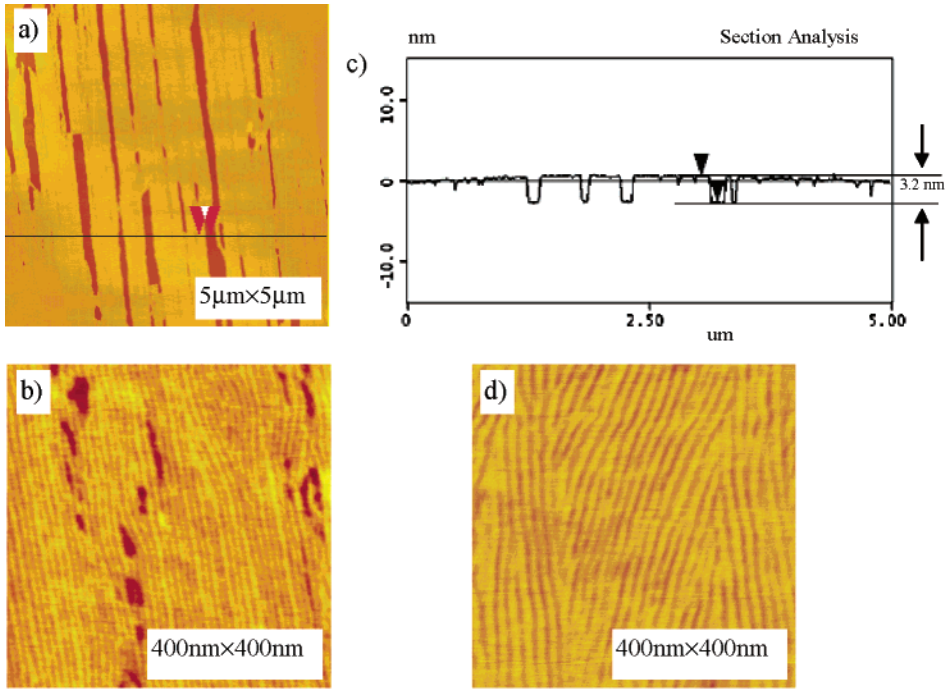

Figure 2. Ex situ AFM images of DPDA-10 micellar structures adsorbed on a mica sheet: (a) large area image; (b) magnified image; (c) section analysis of (a); (d) in situ AFM image of DPDA-10 micellar structures adsorbed on a mica sheet.

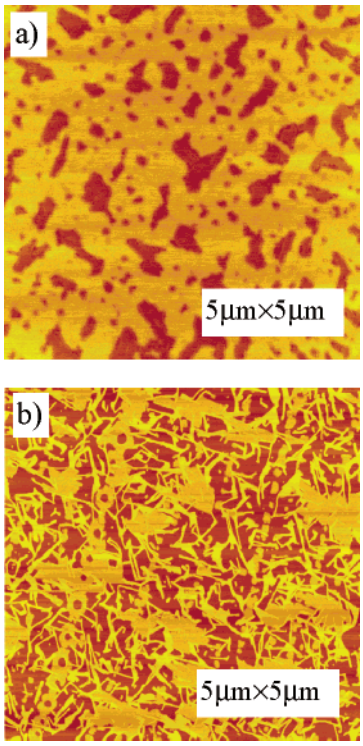

Figure 3. Ex situ AFM observation of the self-organized structure of DPDA with the different spacers: (a) DPDA-7; (b) DPDA-15.

over time, and concomitantly, the absorption in the longer-wavelength region (350−600 nm) increases gradually. There is an isosbestic point at about 370 nm. The spectra change indicates that the polymerization has taken place and the polymer with a higher conjugation length is formed.[12] From 50 min later on (data not shown), the spectra change little upon UV irradiation, indicating that most of the molecules are polymerized. In this procedure, the DPDA-10 aqueous solution turns from colorless to yellow, which is also a symbolic phenomenon of the polymerization of diacetylene. It should be noted that diacetylene

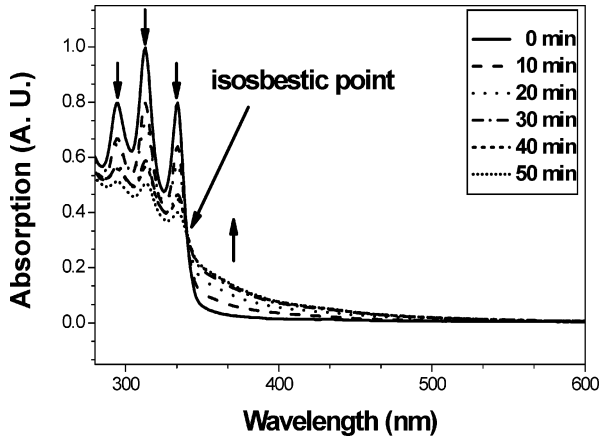

Figure 4. Dependence of the UV−vis absorption spectrum of the DPDA-10 solution on UV light irradiation time.

has two modes of polymerization: one is 1,4-addition, which will generate a new strong absorption band at around 500−700 nm; the other is 1,2-addition, which has no distinct absorption band, but there is an absorption band at around 350−600 nm that increases gradually with the extension of irradiation time. In our case, the polymerization of diacetylene occurs with 1,2-addition.[12]

This polymerization process could also be evidenced by the FTIR spectra. As depicted in the FTIR spectrum in Figure 5, the DPDA-10 monomer (Figure 5, solid curve) shows the characteristic absorption bands at 2213 (asymmetric) and 2147 (symmetric) cm^{-1} assigning to the stretching vibration of the C≡C bonds in symmetrically substituted diacetylene. After UV irradiation (Figure 5, dashed curve), the asymmetric vibration absorption band at 2213 cm^{-1} almost disappears, and the

(12) (a) Fomina, L.; Allier, H.; Fomine, S.; Salcedo, R.; Ogawa, T. *Polym. J.* **1995**, *27*, 591. (b) Barentsen, H. M.; Dijk, M.; Kimkes, P.; Zuilhof, H.; Sudhoelter, E. J. R. *Macromolecules* **1999**, *32*, 1753. (c) Tachibana, H.; Yamanaka, Y.; Sakai, H.; Abe, M.; Matsumoto, M. *Macromolecules* **1999**, *32*, 8306. (d) Lee, J. H.; Curtis, M. D.; Kampf, J. W. *Macromolecules* **2000**, *33*, 2136. (e) Iwase, Y.; Kondo, K.; Kamada, K.; Ohta, K. *J. Polym. Sci., Part A: Polym. Chem.* **2001**, *39*, 3686.

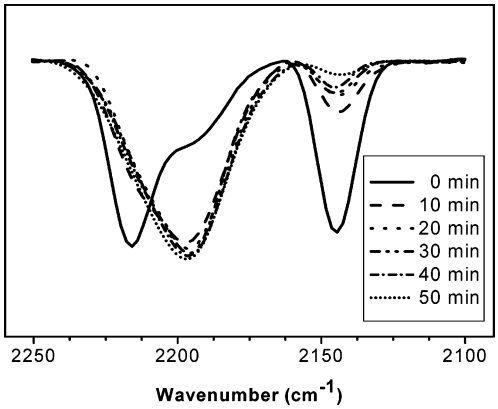

Figure 5. Dependences of the FTIR spectrum of the DPDA-10 solution on UV light irradiation time.

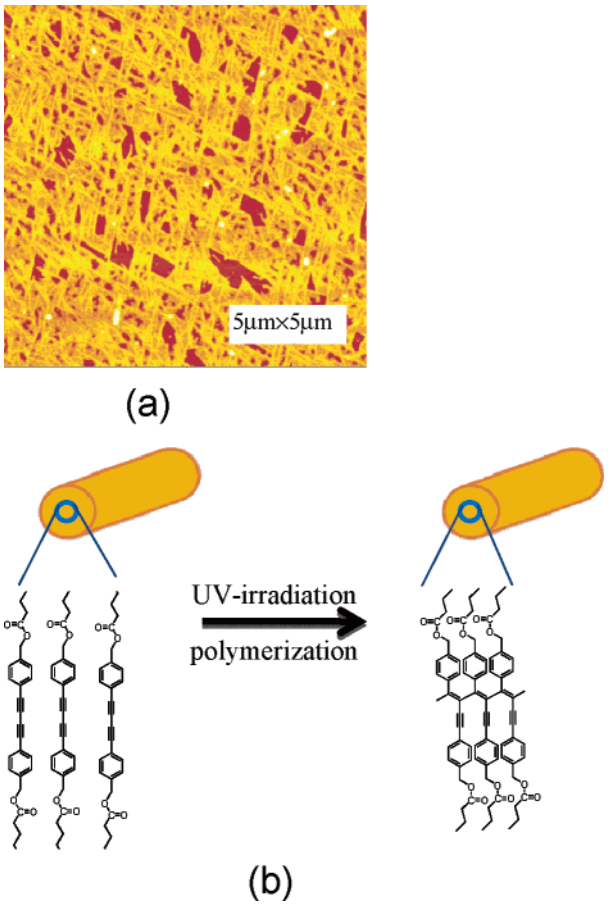

Figure 6. (a) Ex situ AFM observation of the self-organized structure of the polymerized DPDA-10 at the mica/water interface. (b) Plausible structure change of the DPDA-10 before and after polymerization.

symmetric vibration absorption band at 2147 cm^{-1} decreases dramatically. Simultaneously, a new absorption band at 2197 cm^{-1} (the asymmetric stretching vibration of the C≡C bonds) appears, suggesting that polymerization has taken place, indeed.[12a,d] From the UV−vis and FTIR spectra, we conclude that DPDA-10 in the self-organized assemblies can be polymerized, which may not only help for stabilizing the micellar structure but also provide good optical and electronic properties due to the elongation of the π-conjugation caused by polymerization.

The Self-Assemblies Can Still Keep Their Structure after Polymerization. We then come to a question regarding whether the assemblies are robust enough to withstand polymerization. In other words, we are wondering whether the micelles can maintain their cylindrical structure in this procedure. To clarify

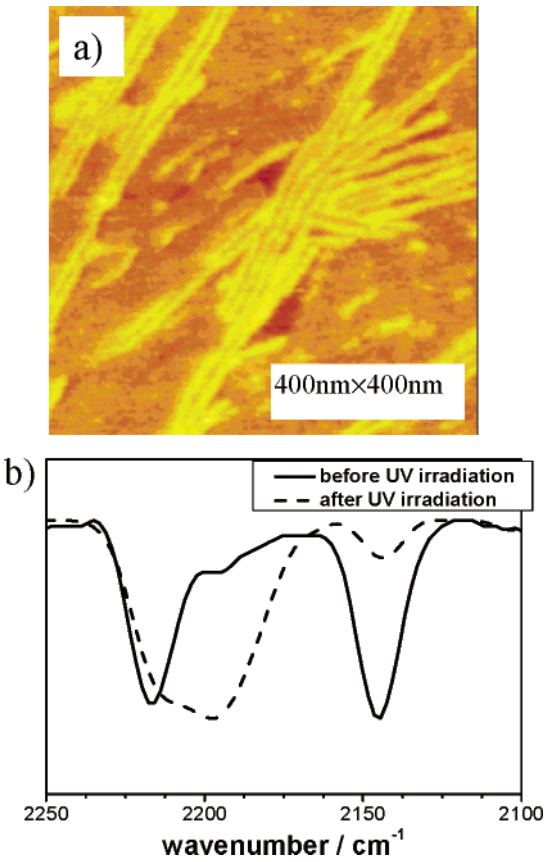

Figure 7. The morphology and polymerization characterization of the DPDA-10 micelles at the mica/water interface after UV irradiation. (a) In situ AFM observation of the self-organized structure of the DPDA-10 micelles at the mica/water interface after UV irradiation. (b) FTIR spectra of DPDA-10 before (solid line) and after the UV-irradiation (dash line). The samples were dropped onto CaF_2 and dried before recording.

this question, we observed the morphology of the polymerized structure as in observing the self-organized aggregates. A mica sheet was put into the polymerized solution allowing for the adsorption, taken out and air-dried, then imaged by ex situ AFM observation. As shown in Figure 6a, the cylindrical micellar structures can also observed, indicating that the cylindrical micellar structures formed by DPDA-10 can be preserved during the UV irradiation-induced polymerization in the solution. Here, Figure 6b shows the plausible structure change of the DPDA-10 before and after polymerization.

Since the cylindrical micellar structures formed by DPDA-10 can be preserved in its polymerization solution, we also want to clarify whether the surface micelles can keep their cylindrical morphology at the surface after UV irradiation. The mica sheet with preformed micellar structures of DPDA-10 was irradiated by a UV fiber lamp for 10 min under argon atmosphere. After polymerization, the sample was observed by in situ AFM in the polymerized DPDA-10 solution. From the in situ AFM image (Figure 7a), the cylindrical micellar structures at the mica/water interface were preserved after polymerization. To confirm the polymerization of the DPDA-10 surface micelles at the interface, we also used FTIR to characterize the polymerized surface micelles. The DPDA-10 solution was dripped onto CaF_2 and air-dried at room temperature, then irradiation for 10 min under argon atmosphere with a UV fiber lamp before the FTIR observation. As shown in Figure 7b, the absorption band at 2213 cm^{-1} almost disappears and that at 2147 cm^{-1} decreases drastically, and a new absorption band at 2197 cm^{-1} appears

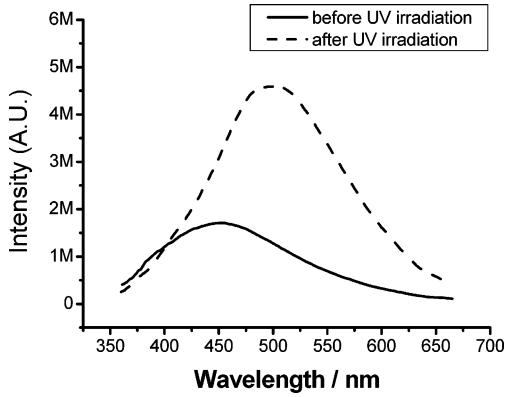

Figure 8. Fluorescence spectra of the DPDA-10 solution before (solid line) and after UV irradiation (dashed line) upon excitation at 394 nm.

after UV irradiation, just the same as the observation of polymerization in the solution.

Emission Property of the Polymerized Nanostructures. We wondered whether the introduction of polydiacetylene can increase the function of the micellar nanomaterials, e.g., emission property. To answer this question, we observed the emitting properties of the 1.0×10^{-3} M DPDA-10 solutions before and after UV irradiation by measuring the fluorescence emission spectra. As shown in Figure 8, the emission spectrum of DPDA-10 solution before UV irradiation shows a maximum fluorescence peak at 448 nm (Figure 8, solid curve), originating from the emission of the conjugated diphenylbutadiynyl group. However, the fluorescence maximum is considerably red-shifted from 448 to 497 nm, and the fluorescent intensity is significantly increased, about four times more than that before UV irradiation (Figure 8, dashed curve). We have also measured the emission spectra of the film formed by dropping the UV-irradiated and nonirradiated solution onto quartz slides, and both spectra are similar to that obtained by directly measuring the emission of the solution. (Supporting Information Figure S1). The red shift and increase of the intensity in the fluorescence after UV irradiation may arise from the extension of the conjugated system upon polymerization. Thus, the introduction of polydiacetylene can enhance the optical property of the micellar nanomaterials.

Conclusion

We have designed and synthesized three polymerizable bolaamphiphiles with different lengths of alkyl chain containing a cationic pyridinium head group at each end of the alkyl chain and a mesogenic diphenylbutadiynyl unit. DPDA-10 with an appropriate length of the flexible spacer can self-organize into stable cylindrical nanosized structures. The DPDA-10 micelles can be photopolymerized both in the bulk solution and in the film by UV irradiation, and the cylindrical structure of the DPDA-10 micelles at the mica/water interface can be preserved after UV-irradiation polymerization. Two phenyl ring side substituents directly conjugated to the polydiacetylene main chain can significantly enhance the emission property of the polymerized DPDA-10 micelles compared with that of unpolymerized DPDA-10 micelles. Thus, this work may provide a new approach for designing well-ordered nanomaterials and fabricating good optical property of organic functional nanostructure materials.

Acknowledgment. The authors thank the National Basic Research program of China (2007CB808000, 2005CB724400), the National Natural Science Foundation of China (20574040, 20334010, 20473045), the Postdoctoral Science Foundation of China (20060390055), and the Ministry of Education for financial supports.

Supporting Information Available: Emission spectra of DPDA-10 adsorbed onto quartz slides before and after polymerization, and UV−vis spectra of DPDA-10 in CH_3OH and in water, respectively. This material is available free of charge via the Internet at http://pubs.acs.org.

LA700281F